

High-Output-Power Single-Higher-Order Transverse Mode VCSEL With Shallow Surface Relief

Abdel-Sattar Gadallah and Rainer Michalzik

Abstract—We report high-power single-higher-order transverse mode emission of a large-area oxide-confined rectangular-shaped vertical-cavity surface-emitting laser (VCSEL) with a multispot shallow surface relief. Both a record-high output power of 12 mW and a record-low differential series resistance of 18 Ω are achieved. Stable single-higher-order transverse mode emission with a side-mode suppression ratio (SMSR) exceeding 35 dB is maintained up to thermal rollover. Single-polarization lasing along the major axis is achieved with 27.5-dB spectral orthogonal polarization suppression ratio at thermal rollover. Measurements of near- and far-field intensity profiles of the higher-order mode are also presented.

Index Terms—Higher-order mode, polarization control, single-mode, vertical-cavity surface-emitting laser (VCSEL).

I. INTRODUCTION

THE appealing attributes of single-mode vertical-cavity surface-emitting lasers (VCSELs) such as spectral purity and tailored near-field and far-field intensity profiles promote VCSEL applications in, e.g., spectroscopy, sensing or biophotonics. While single longitudinal mode emission is an inherent VCSEL feature, their large transverse dimensions usually induce multiple transverse mode oscillation. The straightforward approach to design a single fundamental transverse mode VCSEL is to reduce its transverse dimension, thus preventing the propagation of higher-order modes, in analogy to single-mode fiber theory [1]. However, this simple technique imposes an upper limit of about 4 μm on the active diameter of an oxide-confined VCSEL. Such small-area lasers have low output powers, high differential series resistances, tight fabrication tolerances, and potentially reduced lifetimes due to high current densities. The maximum output power P_{max} thus achieved is typically less than 5 mW and the differential series resistance is higher than 100 Ω [2]. Different approaches have been taken to obtain a higher P_{max} by utilizing a larger active diameter. These include the spatial modification of the laser cavity with a surface relief [3]–[5], coupled resonators [6], employing zinc diffusion in the top mirror [7] and compact vertical extended-cavity surface-emitting lasers (VECSELs) [8]. However, these methods either provide $P_{\text{max}} \leq 7.5$ mW

Manuscript received July 27, 2010; revised March 16, 2011; accepted April 30, 2011. Date of publication May 27, 2011; date of current version July 07, 2011.

A.-S. Gadallah was with the Institute of Optoelectronics, Ulm University, Ulm, Germany. He is now with the Department of Laser Sciences and Interactions, National Institute of Laser Enhanced Sciences, Cairo University, 12613 Giza, Egypt (e-mail: agadallah@niles.edu.eg).

R. Michalzik is with the Institute of Optoelectronics, Ulm University, 89069 Ulm, Germany (e-mail: rainer.michalzik@uni-ulm.de).

Color versions of one or more of the figures in this letter are available online at <http://ieeexplore.ieee.org>.

Digital Object Identifier 10.1109/LPT.2011.2152388

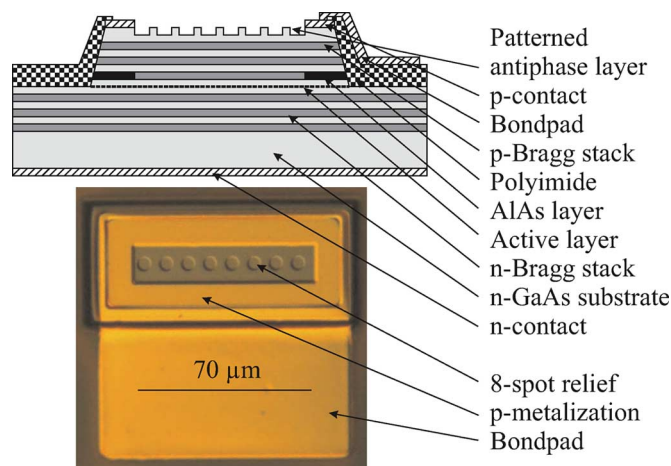


Fig. 1. Schematic drawing (top) and photograph (bottom) of a fully processed eight-spot shallow surface-etched rectangular-shaped VCSEL.

[3]–[7] or require rather complicated fabrication steps [8]. An alternative approach is to select a single high-order transverse mode [9], [11]. Such devices can have larger active areas. Maximum continuous-wave (CW) output powers of about 7.5 mW in the fundamental mode [5] and about 7 mW in a high-order mode [9] have been obtained from VCSELs with circular shape. In this letter, we report a VCSEL design with an oblong-shaped aperture and mode selection through multispot surface etching in an antiphase layer above the top distributed Bragg reflector. The output power extracted from the device is about 12 mW in a single high-order mode. To our knowledge, this is the highest power in a single mode from any fully monolithic VCSEL. Moreover, the large aperture area results in a differential series resistance of only 18 Ω . The devices can be applied for, e.g., optical particle manipulation in microfluidics using light forces [10].

II. DESCRIPTION OF THE DEVICE

Fig. 1 shows a schematic and a photograph of an eight-spot surface-etched rectangular-shaped VCSEL to enforce single-mode operation of the E_{81} mode having 8 intensity maxima along the aperture length and one maximum along the aperture width. The epitaxial material was provided by Philips Technologie GmbH U-L-M Photonics. The layer structure consists of a bottom n-doped 37-pairs distributed Bragg reflector (DBR), a one-wavelength thick cavity containing three 8 nm thick GaAs quantum wells separated by 10 nm AlGaAs barriers, a 22-pairs p-DBR and a topmost quarter-wave thick GaAs antiphase layer, all grown on an n-GaAs substrate. The cavity resonance is in the vicinity of 850 nm. The antiphase layer induces extra losses. This layer is spatially selectively removed in a single processing step using wet-chemical etching. The eight-spot shallow etch

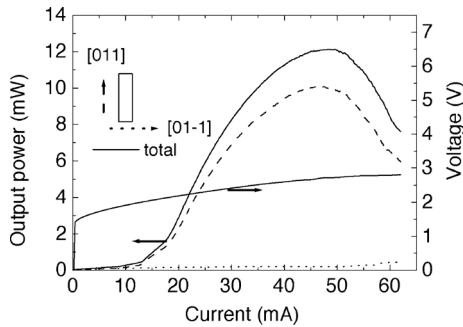


Fig. 2. CW polarization-resolved light-current characteristics as well as current-voltage curve of an eight-spot surface relief VCSEL with an active aperture area of $6.3 \times 68.3 \mu\text{m}^2$.

pattern in Fig. 1 is adapted to the intensity profile of the E_{81} mode. The diameter of each spot is about $6 \mu\text{m}$, the pitch is $D = 9 \mu\text{m}$ and the active aperture area is about $6 \mu\text{m} \times 68 \mu\text{m}$. The pattern is designed such that there is a maximum overlap between the etched spots and the calculated intensity maxima of the targeted mode. The function of this maximum overlap is twofold: Not only does it decrease the threshold gain of the targeted mode, but it also increases the output power emitted from the device. With this method, a single-higher-order transverse mode is selected. The analysis of higher-order-mode selection using surface etching is reported in [12]. Current confinement is achieved through thermal oxidation of an AIAs layer placed just above the one-wavelength thick inner cavity. This step defines the aperture area mentioned above. Wet etching is used to reach the AIAs layer. N- and p-type metalization processes are applied, followed by polyimide passivation. Finally, bondpad metalization is carried out for electrical contacting.

III. CHARACTERIZATION AND RESULTS

Room temperature CW light-current-voltage characteristics of a VCSEL with the pattern and aperture area described above are shown in Fig. 2. Polarization-resolved light-current curves have been taken by inserting a Glan-Thompson polarizer in front of the photodetector. The total power curve (full line) shows that the maximum output power is $P_{\text{max}} = 12 \text{ mW}$ at 48 mA current. The average differential series resistance is 18Ω , as obtained from the slope of the current-voltage curve in the range from 20 to 50 mA. The threshold current of $I_{\text{th}} = 12.8 \text{ mA}$ is relatively high due to the losses induced by the antiphase layer. The maximum differential quantum efficiency is $\eta_d = 38.5\%$.

The dashed and dotted lines in Fig. 2 reveal that the emission is dominantly polarized along the aperture length. The orthogonal polarization suppression ratio is 17 dB at thermal rollover. Since the difference between the total output power and the dominant polarization is due to optical losses of the polarizer, the maximum single-mode, single-polarization output power takes a record-high value of about 12 mW.

Emission spectra at different currents were taken with an optical spectrum analyzer (OSA) with 10 pm resolution and are displayed in Fig. 3. The laser light was coupled into a $50 \mu\text{m}$ core diameter graded-index multimode fiber for signal input to the OSA. The competitive mode is suppressed by 35 dB versus the targeted mode up to the thermal rollover point at about 50 mA current. Polarization-resolved spectra of the device

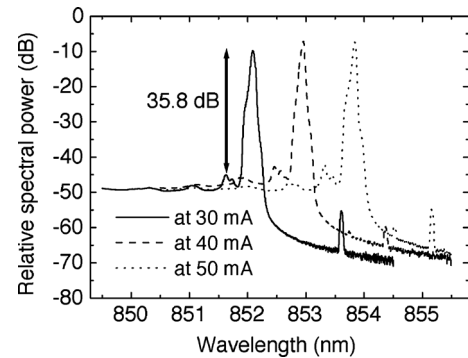


Fig. 3. Emission spectra of the device from Fig. 2 at different currents.

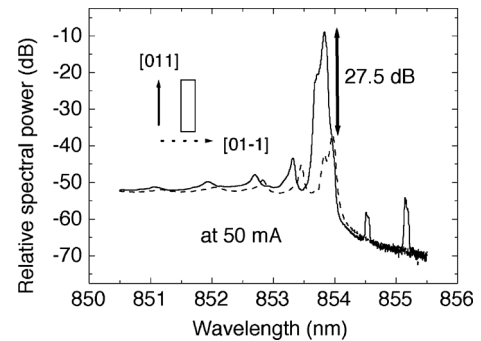


Fig. 4. Polarization-resolved spectra at 50-mA current, corresponding to Figs. 2 and 3.

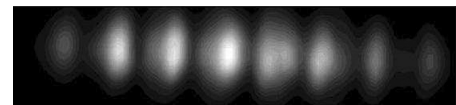


Fig. 5. Near-field intensity profile of the device from Fig. 2 at 30 mA. The scan area is $68 \mu\text{m} \times 16 \mu\text{m}$.

are shown in Fig. 4. At 50 mA, the peak spectral intensity of the selected polarization parallel to the aperture length is 27.5 dB higher than that of the polarization along the aperture width.

The main spectral peaks in Figs. 3 and 4 contain a shoulder which might indicate the presence of an additional, less strongly suppressed mode. In VCSELs, spectrally very closely spaced modes are often almost degenerate modes with identical mode order but orthogonal polarization. The polarization-resolved spectra in Fig. 4 prove that the shoulder in the main peak cannot contain such an orthogonal mode. To identify the order of the main mode, we have performed spectrally resolved near-field measurements by scanning a lensed single-mode fiber tip over the output aperture with high spatial resolution. The emitted spectrum is collected at each lateral scan position. The data can then be numerically filtered in the spectral domain and represented in a spatially two-dimensional plot. Fig. 5 shows such a near-field intensity profile of the VCSEL from Fig. 3 at 30 mA, taken with a spectral width of 0.046 nm centered around the spectral peak. In this case, the filter width excludes the spectral shoulder. On the other hand, no changes of the profile are observed even with 5 nm spectral width, where the contributions of all other modes are included. Since we have observed similar shoulders in the spectra of purely single-mode small-area circular VCSELs, we attribute them to the multimode fiber input of the OSA. Especially with the given high-order asymmetric VCSEL mode in Fig. 5, a lot of high-order fiber modes are excited, which lead to different

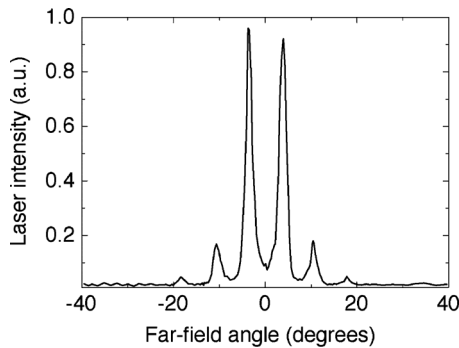


Fig. 6. Measured far-field intensity profile corresponding to Fig. 5.

free-space propagation (compared to a single-mode fiber input) inside the OSA between fiber and diffraction grating.

In contrast to the simulations of the field pattern, in Fig. 5 there is a marked difference between the intensity maxima and shape of the spots. We attribute this to the inhomogeneous temperature throughout the active aperture, which leads to cavity detuning. We believe that layer thickness variations resulting from the epitaxial growth can be neglected here. In fact we have obtained much less distinct mode shapes and much lower powers with more inhomogeneous wafer material.

Fig. 6 shows the measured far-field intensity in the plane defined by the etch spots. Four major peaks are observed. To very good accuracy, the diffraction peaks of order m are found at angles $\sin \theta = (2m - 1)\lambda/(2D)$, as expected for a linear array of emitting apertures with a phase difference of π between the fields of nearest neighbors ([13], Sect. 10.7). This model is a rather good representation since the expected ideal electric field profile of the selected E_{81} mode is very similar to a sine function with four maxima and four minima. The data are: $(m, \theta_{\text{theory}}(^{\circ}), \theta_{\text{experiment}}(^{\circ})) = (1, 2.7, 3.1), (2, 8.2, 8.4), (3, 13.7, 14.0)$.

In a standard VCSEL corresponding to Fig. 2, the antiphase layer is removed over the entire p-contact opening. Such a laser has parameters $I_{\text{th}} = 7$ mA, $P_{\text{max}} = 34$ mW at thermal rollover, and $\eta_d = 51\%$. However, the emission spectrum shows a multitude of transverse modes with a spectral width exceeding 1 nm. Clearly there is a trade-off between I_{th} , P_{max} , η_d and the spectral purity of these laser types. Optical absorption losses in the GaAs antiphase layer (which is the same material as the quantum wells), stronger device heating, and higher carrier losses are likely reasons for the reduced η_d of the single-mode VCSEL.

Within our studies, surface-etched VCSELs with different geometry have been investigated. Lasers with an aperture area of $6.3 \times 68.3 \mu\text{m}^2$ as in Fig. 2 but 10 etch spots, each with $5 \mu\text{m}$ diameter have $I_{\text{th}} = 16.7$ mA and emit the E_{101} mode with $P_{\text{max}} \approx 10$ mW and SMSR ≈ 35 dB. A smaller device with a size of $6 \times 30 \mu\text{m}^2$ and a four-spot relief with $4 \mu\text{m}$ diameter has $I_{\text{th}} = 9.6$ mA and $P_{\text{max}} = 4$ mW in the E_{41} mode at thermal rollover with SMSR ≈ 30 dB.

IV. CONCLUSION

We have demonstrated that large-area ($>400 \mu\text{m}^2$) multipot surface-etched rectangular-shaped VCSELs show stable

high-power single-higher-order transverse mode emission. Moreover, the differential series resistance is low. Near- and far-field intensity profiles prove the successful mode selection. Besides, the oblong geometry of the device favors emission with a stable linear polarization, as observed before for other geometries [14], [15]. The manufacturing of this VCSEL needs only one additional lithography and etching step, which makes it attractive for commercial fabrication.

ACKNOWLEDGMENT

The authors would like to thank R. Rösch for the evaporation of n- and p-type contact metals and Philips Technologie GmbH U-L-M Photonics, Ulm, Germany for providing the excellent wafer material.

REFERENCES

- [1] A. W. Snyder and J. D. Love, *Optical Waveguide Theory*. London: Chapman & Hall, 1991.
- [2] C. Jung, R. Jäger, M. Grabherr, P. Schnitzer, R. Michalzik, B. Weigl, S. Müller, and K. J. Ebeling, "4.8 mW singlemode oxide confined top-surface emitting vertical cavity laser diode," *Electron. Lett.*, vol. 33, no. 21, pp. 1790–1791, 1997.
- [3] Å. Haglund, J. Gustavsson, J. Vukušić, P. Modh, and A. Larsson, "Single fundamental mode output power exceeding 6 mW from VCSELs with a shallow surface relief," *IEEE Photon. Technol. Lett.*, vol. 16, no. 2, pp. 368–370, Feb. 2004.
- [4] A. Kroner, F. Rinaldi, J. Ostermann, and R. Michalzik, "High-performance single fundamental mode AlGaAs VCSELs with mode-selective mirror reflectivities," *Opt. Commun.*, vol. 270, no. 2, pp. 332–335, 2006.
- [5] A. Furukawa, S. Sasaki, M. Hoshi, A. Matsuzono, K. Moritoh, and T. Baba, "High-power single-mode vertical-cavity surface-emitting lasers with triangular holey structure," *Appl. Phys. Lett.*, vol. 85, no. 22, pp. 5161–5163, 2004.
- [6] A. J. Fischer, K. D. Choquette, W. W. Chow, A. A. Allerman, D. K. Serkland, and K. M. Geib, "High single-mode power observed from a coupled-resonator vertical-cavity laser diode," *Appl. Phys. Lett.*, vol. 79, no. 25, pp. 4079–4081, 2001.
- [7] J.-W. Shi, C.-C. Chen, Y.-S. Wu, S.-H. Guo, C. Kuo, and Y.-J. Yang, "High-power and high-speed Zn-diffusion single fundamental-mode vertical-cavity surface-emitting lasers at 850-nm wavelength," *IEEE Photon. Technol. Lett.*, vol. 20, no. 13, pp. 1121–1123, Jul. 1, 2008.
- [8] I. Kardosh, F. Demaria, F. Rinaldi, S. Menzel, and R. Michalzik, "High power single transverse mode vertical-cavity surface-emitting lasers with monolithically integrated curved dielectric mirrors," *IEEE Photon. Technol. Lett.*, vol. 20, no. 24, pp. 2084–2086, Dec. 15, 2008.
- [9] P. R. Claisse, W. Jiang, P. A. Kiely, B. Gable, and B. Koonse, "Single high order mode VCSEL," *Electron. Lett.*, vol. 34, no. 7, pp. 681–682, 1998.
- [10] A. Gadallah, A. Bergmann, and R. Michalzik, "High-power single-higher-order-mode VCSELs for optical particle manipulation," *Proc. SPIE*, vol. 7720, pp. 77201Y-1–77201Y-10, 2010.
- [11] S. Shinada and F. Koyama, "Single high-order transverse mode surface-emitting laser with controlled far-field pattern," *IEEE Photon. Technol. Lett.*, vol. 14, no. 12, pp. 1641–1643, Dec. 2002.
- [12] A. Gadallah, A. Kroner, I. Kardosh, F. Rinaldi, and R. Michalzik, "Ob-long-shaped VCSELs with pre-defined mode patterns," *Proc. SPIE*, vol. 6997, pp. 69971R-1–69971R-9, 2008.
- [13] K. J. Ebeling, *Integrated Optoelectronics*. Berlin: Springer-Verlag, 1993.
- [14] K. D. Choquette and R. Leibenguth, "Control of vertical cavity laser polarization with anisotropic transverse cavities," *IEEE Photon. Technol. Lett.*, vol. 6, no. 1, pp. 40–42, Jan. 1994.
- [15] P. Debernardi, H. J. Unold, J. Maehns, R. Michalzik, G. B. Bava, and K. J. Ebeling, "Single-mode, single-polarization VCSELs via elliptical surface etching: Experiments and theory," *IEEE J. Sel. Topics Quantum Electron.*, vol. 9, no. 5, pp. 1394–1404, Sep./Oct. 2003.